ACS APPLIED MATERIALS & INTERFACES
Research Article
www.acsami.org

Low-Temperature Growth of Indium Oxide Thin Film by Plasma-Enhanced Atomic Layer Deposition Using Liquid Dimethyl(*N*-ethoxy-2,2-dimethylpropanamido)indium for High-Mobility Thin Film Transistor Application

Hyo Yeon Kim,[†,‡] Eun Ae Jung,[†,§] Geumbi Mun,[∥] Raphael E. Agbenyeke,[†,⊥] Bo Keun Park,[†,⊥] Jin-Seong Park,[‡] Seung Uk Son,[§] Dong Ju Jeon,[†] Sang-Hee Ko Park,[∥] Taek-Mo Chung,[*,†,⊥] and Jeong Hwan Han[*,†,⊥]

[†]Division of Advanced Materials, Korea Research Institute of Chemical Technology(KRICT), 141 Gajeong-Ro, Yuseong-Gu, Deajeon 34114, Republic of Korea

[‡]Division of Materials Science and Engineering, Hanyang University, 222 Wangsimni-Ro, Seoul 04763, Republic of Korea

[§]Department of Chemistry, Sungkyunkwan University, Suwon 16419, Republic of Korea

[∥]Department of Materials Science and Engineering, Korea Advanced Institute of Science and Technology (KAIST), 291 Daehak-ro, Yuseong-gu, Daejeon, 34141, Republic of Korea

[⊥]Department of Chemical Convergence Materials, University of Science and Technology (UST), 217 Gajeong-Ro, Yuseong-Gu, Deajeon 34113, Republic of Korea

Supporting Information

Downloaded via KOREA ADVANCED INST SCI AND TECHLGY on November 26, 2019 at 08:17:33 (UTC).
See https://pubs.acs.org/sharingguidelines for options on how to legitimately share published articles.

ABSTRACT: Low-temperature growth of In_2O_3 films was demonstrated at 70−250 °C by plasma-enhanced atomic layer deposition (PEALD) using a newly synthesized liquid indium precursor, dimethyl(*N*-ethoxy-2,2-dimethylcarboxylicpropanamide)indium ($Me_2In(EDPA)$), and O_2 plasma for application to high-mobility thin film transistors. Self-limiting In_2O_3 PEALD growth was observed with a saturated growth rate of approximately 0.053 nm/cycle in an ALD temperature window of 90−180 °C. As-deposited In_2O_3 films showed negligible residual impurity, film densities as high as 6.64−7.16 g/cm^3, smooth surface morphology with a root-mean-square (RMS) roughness of approximately 0.2 nm, and semiconducting level carrier concentrations of 10^{17}−10^{18} cm^{-3}. Ultrathin In_2O_3 channel-based thin film transistors (TFTs) were fabricated in a coplanar bottom gate structure, and their electrical performances were evaluated. Because of the excellent quality of In_2O_3 films, superior electronic switching performances were achieved with high field effect mobilities of 28−30 and 16−19 cm^2/V·s in the linear and saturation regimes, respectively. Furthermore, the fabricated TFTs showed excellent gate control characteristics in terms of subthreshold swing, hysteresis, and on/off current ratio. The low-temperature PEALD process for high-quality In_2O_3 films using the developed novel In precursor can be widely used in a variety of applications such as microelectronics, displays, energy devices, and sensors, especially at temperatures compatible with organic substrates.

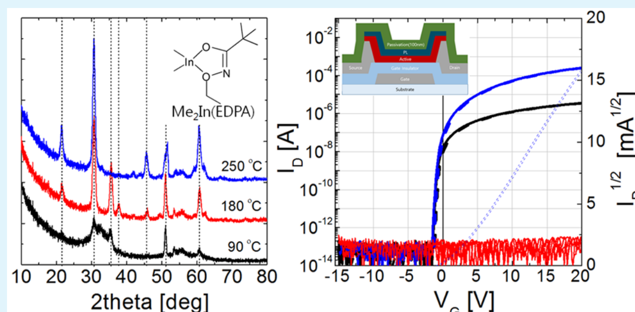

KEYWORDS: *novel indium precursor, indium oxide, low-temperature plasma-enhanced atomic layer deposition, high-mobility thin film transistor*

INTRODUCTION

To realize superhigh-vision, high-frame-rate, large-area, and 3D display technologies, it is necessary to develop high-mobility thin film transistors (TFTs) with field effect mobilities as high as 20−30 cm^2/V·s and good electrical stability, and thus they have been extensively investigated.[1−3] Of the many issues that must be considered to achieve the TFT performance described above, the growth of a high-quality oxide semiconductor film that acts as a conducting channel between the source and drain is decisive. Among the oxide semiconductors available, indium (In)-containing oxide thin films, such as In_2O_3, $InZnO_x$, $InSnO_x$, and $InGaZnO_x$, have been studied extensively as n-channel layers because the large overlap of the In 5s orbital can provide a facile electron transport path with a low electron effective mass.[4−8] In particular, a binary In_2O_3 layer has great potential in various applications because of its superior electron

Received: June 16, 2016
Accepted: September 7, 2016
Published: September 27, 2016

ACS Publications © 2016 American Chemical Society

DOI: 10.1021/acsami.6b07332
ACS Appl. Mater. Interfaces 2016, 8, 26924−26931

conducting properties and wide band gap (3.6−3.8 eV).[9] Moreover, composition control of binary In_2O_3 films is easier than that of ternary and quaternary oxide semiconductors. Meanwhile, In_2O_3 films are known to contain relatively high levels of oxygen defect densities because of the rather low cation-oxygen bond dissociation energy of 346 kJ/mol, and consequently features high electron density levels of 10^{19}−10^{21} cm^{-3}.[10] Therefore, it is necessary to achieve high-quality In_2O_3 film with a suppressed carrier density about 10^{17}−10^{18} cm^{-3} to use a binary In_2O_3 film as an electric field effect channel layer.

Many deposition methods have been explored for the growth of In_2O_3 thin films, including sol−gel processing, sputtering, evaporation, chemical vapor deposition (CVD), and atomic layer deposition (ALD).[9,11−13] In particular, ALD has been widely employed to produce high-quality films based on the self-limited surface chemical reaction between the metal precursor and the reactant. Generally, because not only the resultant film properties but also the ALD process conditions are strongly determined by the intrinsic nature of the metal precursor itself, many In precursors have been synthesized and evaluated in combination with different reactants. $InCl_3$ was first explored with H_2O and yielded transparent films with a resistivity of 3×10^{-3} Ω·cm.[14] However, a relatively low growth rate of <0.027 nm/cycle at a high deposition temperature of 400−500 °C was observed because of the low chemical reactivity of $InCl_3$ toward H_2O. Furthermore, $InCl_3/H_2O$ chemistry produced corrosive HCl byproducts during In_2O_3 growth, which led to damage to the deposition tool and the In_2O_3 film itself. Metal−organic (MO) precursors were also investigated to obtain In_2O_3 films at higher growth rates and lower deposition temperatures. $In(acac)_3/H_2O$ (acac = acetylacetonate) and $In(acac)_3/O_3$ were considered at growth temperatures of 165−200 and 165−225 °C, respectively, but, unfortunately, a clear self-limiting reaction was not found.[15] Trimethylindium (TMIn) and H_2O showed self-limiting In_2O_3 growth with a deposition rate of 0.039 nm/cycle in a temperature range of 200−250 °C.[16] Cyclopentadienylindium-(I) (InCp) showed very low growth rates below 0.02 nm/cycle when solely H_2O or O_2 reactant was used as the oxidant, whereas a much improved growth rate of 0.16−0.2 nm/cycle was achieved when O_3 was introduced.[17,18] Ramachandran et al. reported that plasma-enhanced atomic layer deposition (PEALD) In_2O_3 using $In(tmhd)_3$ (tmhd = 2,2,6,6-tetramethyl-3,5-heptanedionate) and O_2 plasma exhibited a low growth rate of 0.014 nm/cycle with a wide growth temperature range of 100−400 °C.[19] However, the use of the In precursors described above in industrial ALD equipment had the crucial limitation that these In precursors exist in the solid state at room temperature. Therefore, recent research progress on novel In precursors has focused on the synthesis of liquid In precursors with high chemical reactivity, volatility, and thermal stability for practical applications. Maeng et al. reported In_2O_3 ALD processes using novel liquid In precursors, diethyl[bis-(trimethylsilyl)amido]indium ($Et_2InN(TMS)_2$) and [3-(dimethylamino)propyl]dimethylindium (DADI) with H_2O as the reactant.[20,21] $Et_2InN(TMS)_2/H_2O$ and DADI/H_2O ALD processes led to the deposition of highly conductive films with high carrier concentration levels of $\sim 10^{21}$ cm^{-3} and low resistivities of 10^{-4}−10^{-5} Ω·cm.

In this study, we successfully developed a new class of liquid In precursors with high vapor pressure and chemical reactivity. We report the PEALD of In_2O_3 film using this novel precursor over a wide growth temperature range of 70−250 °C. The chemical, physical, optical, and electrical properties of In_2O_3 PEALD films were thoroughly investigated. Finally, ultrathin In_2O_3 films were implemented in a coplanar structure bottom gate TFT as an active layer, and their electronic performances were evaluated for application in high-mobility TFTs.

■ EXPERIMENTAL SECTION

Synthesis of Novel In Precursors with Alkoxycarboxylic Amide Ligands. New types of bidentate alkoxycarboxylic amide ligands, *N*-methoxypropanamide (MPA), *N*-ethoxy-2-methylpropanamide (EMPA), and *N*-ethoxy-2,2-dimethylpropanamide (EDPA), were introduced to synthesize novel In precursors for ALD as listed in Table 1. We used solid TMIn as a starting material and modified it by substituting a methyl group with one of the new ligands above, as shown in Scheme 1. TMIn in toluene was mixed with one equivalent of the ligands with increasing reaction temperature from −78 to 25 °C. Among three different final complexes of **1**−**3**, In complex **3**, which contained two methyl groups and one EDPA ligand, dimethyl(*N*-ethoxy-2,2-dimethylpropanamido)indium ($Me_2In(EDPA)$), has a colorless liquid state at room temperature with good vaporization, whereas complexes **1** and **2** exist in the solid state. Complex **1** is crystallized as dimer with mixed structures of trigonal bipyramid and tetrahedron. On the other hand, electron ionization mass spectrometry (EI-MS) analysis for complex **3** (m/z = 289) demonstrates the formation of monomeric compound. The production of monomeric liquid-state $Me_2In(EDPA)$ **3** might be attributed to the introduction of bulky ligand that hinders μ_2-O bridging between indium ions. NMR, elemental analysis, EI-MS, and thermal gravity analysis (TGA) results for complex **3** are described in the Supporting Information (Figure S1). At temperatures of 26−800 °C, the TGA curve showed single-step evaporation behavior with a small amount of residue (10 wt %), indicating appropriate features for complex **3** to be used as an ALD precursor. A detailed investigation into the synthesis and properties of this new series of In-precursors will be reported elsewhere. In this study, we selected liquid $Me_2In(EDPA)$ as the In source for PEALD In_2O_3 growth.

Table 1. List of Alkoxycarboxylic Amide Ligands in Complexes 1−3

Complex	Ligand	Ligand structure
1	MPA	[structure]
2	EMPA	[structure]
3	EDPA	[structure]

PEALD of In_2O_3 films and characterization. In_2O_3 films were grown by PEALD in a showerhead-type chamber using $Me_2In(EDPA)$ and O_2 plasma. In_2O_3 PEALD was explored at stage temperatures of 70−250 °C, and the reactor wall and gas line were kept at 75−100 °C. $Me_2In(EDPA)$ was heated to 70 °C to supply sufficient vapor, and its delivery to the reaction chamber was assisted by an Ar carrier gas flow of 100 sccm. Pure O_2 gas at a flow rate of 100 sccm was introduced to generate an O_2 plasma at a plasma power of 300 W. The reactor pressure during the ALD process was maintained at 1.5 Torr by automatic control of a throttle valve. One cycle of In_2O_3 PEALD was performed in four sequential steps: $Me_2In(EDPA)$ pulse, Ar purge, O_2 plasma pulse, and Ar purge.

Spectroscopic ellipsometry (SE, Horiba Jobin Yvon UVISEL) was used to determine the In_2O_3 thickness. Glancing angle X-ray diffraction (GAXRD, SmartLab, Rigaku) was carried out to identify the structural characteristics of the as-deposited In_2O_3 films. The densities of In_2O_3 films grown at 90, 180, and 250 °C were examined by the critical angle of the X-ray reflectivity profiles (XRR, SmartLab, Rigaku). The surface morphology and root-mean-square (RMS)

DOI: 10.1021/acsami.6b07332
ACS Appl. Mater. Interfaces 2016, 8, 26924−26931

Scheme 1. Synthesis of Novel in Complexes 1−3

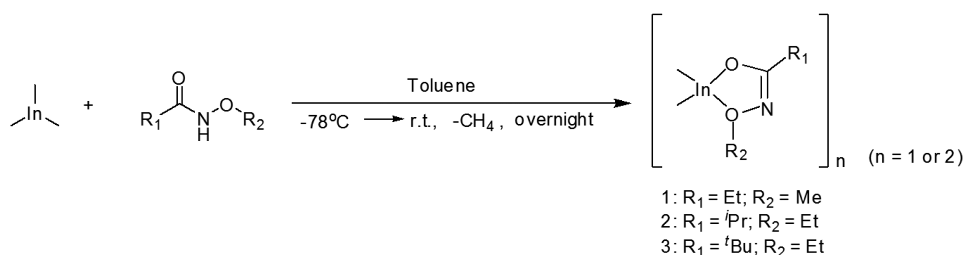

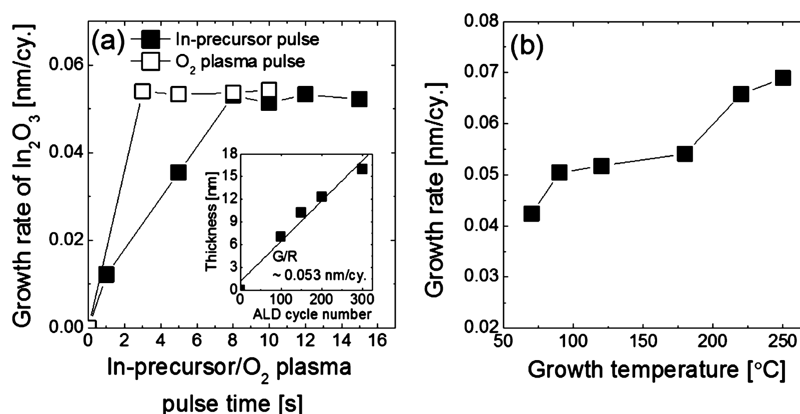

Figure 1. (a) Change in the growth rate of In_2O_3 PEALD with the In precursor and O_2 plasma pulse time. The inset shows the linear growth of the In_2O_3 film at 90 °C with increasing PEALD cycle number. (b) Variation of the In_2O_3 growth rate as a function of the deposition temperature from 70 to 250 °C.

roughness of 19−24 nm-thick In_2O_3 films were confirmed by atomic force microscopy (AFM, DI-3100, Veeco). X-ray photoelectron spectroscopy (XPS, K-Alpha, Thermo Scientific) revealed the chemical binding state of the as-deposited In_2O_3 films and the composition depth profiles for different deposition temperatures. The optical properties including optical transmittance, optical band gap, and refractive index were analyzed using UV−vis spectrophotometry (UV-1800, Shimadzu) and SE. In addition, the electrical properties depending on the growth temperature were studied using Hall measurements (HMS-5000, Ecopia) at room temperature.

Fabrication and Evaluation of In_2O_3-Based TFTs. Ultrathin In_2O_3 PEALD films were applied to the fabrication of coplanar structure bottom-gate TFTs on a glass substrate. For the gate electrode, 150 nm-thick Sn-doped In_2O_3 (ITO) film was grown by sputtering and patterned by photolithography followed by a wet etching process. A gate insulator of 175 nm-thick Al_2O_3 was coated on the gate electrode via ALD using trimethylaluminum (TMA) and H_2O. Next, ITO source and drain electrodes were deposited by sputtering and patterned by photolithography and wet etching. In_2O_3 channel layers as thin as 5 nm were deposited at deposition temperatures of 90, 120, and 180 °C. The representative dimension (width (W) × length (L)) of the channel defined by the patterned source and drain electrodes was 40 μm × 20 μm. Subsequently, the In_2O_3 films were covered by a PEALD Al_2O_3 protecting layer (∼10 nm) prepared from TMA and O_2 plasma and cured in an O_2 atmosphere at 350 °C for 2 h. Finally, the SiO_2 passivation layer (∼100 nm) was deposited using PECVD. Before measuring the electrical properties of the TFT devices, curing annealing was performed again at 300 °C for optimized device performance. Three-terminal current−voltage (CV) curves were obtained using a semiconductor parameter analyzer in a dark probe station chamber at room temperature. The TFT parameters, including turn-on voltage (V_{on}), subthreshold swing (SS), hysteresis (ΔV_{th}), on/off current ratio (I_{on}/I_{off}), and field effect mobilities in the linear and saturation regimes (μ_{lin} and μ_{sat}), were obtained.

■ RESULTS AND DISCUSSION

For In_2O_3 PEALD, $Me_2In(EDPA)$ and O_2 plasma were employed as the In source and oxidant, respectively. In_2O_3 films were grown on Si and glass substrates at deposition temperatures of 70−250 °C. The saturated surface reaction between $Me_2In(EDPA)$ and O_2 plasma was confirmed at a stage temperature of 90 °C, as depicted in Figure 1a. By increasing the $Me_2In(EDPA)$ pulse time from 1 to 15 s, a saturated growth rate of 0.053 nm/cycle could be achieved at In precursor pulse lengths over 8 s. A comparable growth rate about 0.053 nm/cycle was also found by varying the O_2 plasma pulse time within 3−10 s at a fixed In precursor pulse time of 12 s. According to these self-limiting reaction results, the optimal pulse conditions for the PEALD In_2O_3 process were determined to be a 12-s $Me_2In(EDPA)$ pulse, a 10-s Ar purge, a 5-s O_2 plasma pulse, and a 5-s Ar purge. The inset of Figure 1a presents the change in the thickness of the In_2O_3 film as a function of the PEALD cycle number at a deposition temperature of 90 °C. The thickness of In_2O_3 film increased proportionally to the PEALD cycle number, showing the typical linear growth behavior of ALD. The growth rate estimated from the slope was 0.053 nm/cycle, which is consistent with that found from the saturation curves.

The change in the growth rate of In_2O_3 films over a wide deposition temperature range of 70−250 °C was examined, as shown in Figure 1b. At temperatures from 90 to 180 °C, a saturated PEALD growth window was found with an almost constant growth rate of approximately 0.05 nm/cycle. According to our knowledge, the ALD temperature window achieved in this study is at markedly lower temperatures compared to those for previously reported In_2O_3 ALD processes using other In precursors.[14−21] Successful ALD of In_2O_3 films even below 100 °C suggests that this process can be

DOI: 10.1021/acsami.6b07332
ACS Appl. Mater. Interfaces 2016, 8, 26924−26931

adopted for most flexible organic substrates, including polyimide, polyethylenenapthalate, and polyester, for which the maximum process temperature is limited to 300, 150, and 80 °C, respectively.[22] Above 180 °C, higher growth rates of 0.066−0.069 nm/cycle were observed, which might be related to the enhanced kinetics of the surface reaction. It should be noted that the increased growth rate above 180 °C is not related to the thermal decomposition of $Me_2In(EDPA)$. As shown in Figure S2, no film deposition was found when the $Me_2In(EDPA)$ was pulsed without coreactant at the temperatures below 300 °C. However, film formation was observed above 350 °C indicating thermal decomposition of Me_2In-(EDPA) from 350 °C. In addition, we confirmed the self-limiting growth of an In_2O_3 ALD film using $Me_2In(EDPA)$/H_2O chemistry at a high growth temperature of 300 °C, which suggests the sufficient thermal stability of $Me_2In(EDPA)$. A lower growth rate of 0.042 nm/cycle at a deposition temperature of 70 °C might be due to insufficient thermal energy for surface reaction between In precursor and O_2 plasma.

The chemical properties of the In_2O_3 PEALD films were examined using XPS depth profiling and surface analysis.

Figure 2a−c shows the compositional depth profiles for In_2O_3 films deposited at 90, 180, and 250 °C. At these deposition temperatures, In_2O_3 films showed homogeneous In and O profiles in the thickness direction. An insignificant change in In/O atomic ratio was found with varying the deposition temperature. In addition, In_2O_3 films at all deposition temperatures exhibited negligible C and N impurity levels even when the temperature was outside the ALD window (i.e., below 90 °C or over 180 °C), indicating the formation of highly pure In_2O_3 film via the complete removal of ligands by O_2 plasma during PEALD (Figure S3). Impurities below the detection limit for In_2O_3 film grown at 250 °C further supported the absence of thermal decomposition of Me_2In-(EDPA) up to 300 °C, which is consistent with the thermal decomposition test previously described. The low-temperature deposition of In_2O_3 films without C and N impurities is a promising feature of this work. Previously developed liquid In precursors, for example, $Et_2InN(TMS)_2$ and DADI, could produce pure In_2O_3 films at rather high temperatures of 200 and 275 °C, respectively.[20,21] To reveal the chemical binding states of In_2O_3 films grown at 90−250 °C, In 3d and O 1s XP spectra were examined, as depicted in Figure 2d and e. All spectra were calibrated using the binding energy of a C−C bond of 285 eV as a reference and collected after surface sputtering to eliminate the contaminants due to air exposure. The binding energy of the In $3d_{5/2}$ peak for the In_2O_3 film prepared at 90 °C was 444.5 eV, which corresponds to In $3d_{5/2}$ XP spectra of fully oxidized In_2O_3 films.[23] At higher growth temperatures of 180 and 250 °C, the In $3d_{5/2}$ peaks showed lower binding energies of 444.2 and 444.1 eV, respectively. The chemical shift to a lower binding energy might originate from the formation of more oxygen vacancies in the films with increasing growth temperatures for In_2O_3 PEALD. The O 1s peaks of In_2O_3 films deposited at 90−250 °C could be deconvoluted into two contributions; the stronger peaks at a lower binding energy of approx.imately 530 eV are attributed to In−O bonds, whereas the weaker peaks at a higher binding energy correspond to In−OH bonds.

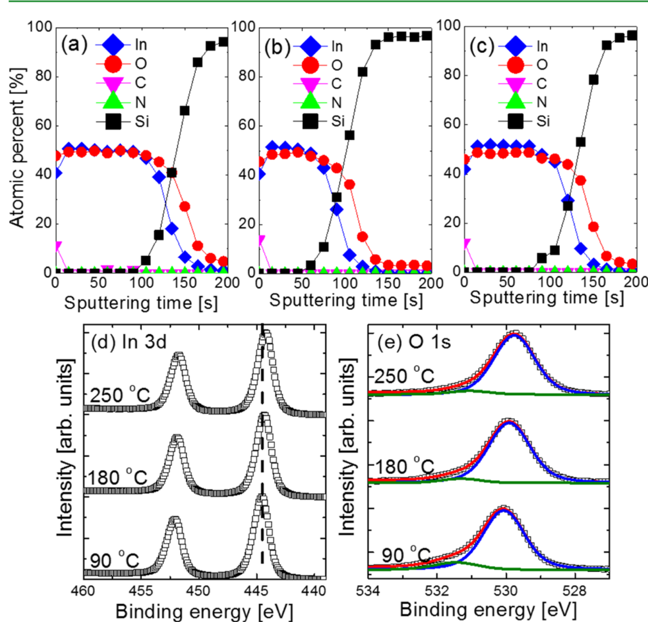

Figure 2. XPS depth profiles of In_2O_3 films grown at (a) 90, (b) 180, and (c) 250 °C. (d) In 3d and (e) O 1s XP spectra of In_2O_3 PEALD films deposited at 90−250 °C.

The crystalline structure of 19−24 nm-thick In_2O_3 PEALD films deposited at stage temperatures of 90−250 °C were investigated by GAXRD, as presented in Figure 3a. The diffraction peaks for all deposition temperatures showed that crystallized In_2O_3 films with a cubic bixbyite structure were achieved as deposited, independent of the growth temperature. At 180 and 250 °C, the (222) diffraction peak at 30.6° is predominant, which agrees well with the XRD patterns of polycrystalline In_2O_3 films fabricated by other deposition methods, such as rf reactive magnetron sputtering, evaporation, and CVD.[11,12] At a lower growth temperature of 90 °C, somewhat broader and weaker diffraction peaks were observed, perhaps because of the formation of In_2O_3 films with smaller grains. In this study, since ultrathin In_2O_3 films were implemented as the channel layer of TFTs, the microstructural characteristics of 5 nm-thick In_2O_3 films deposited at 90 and 250 °C were also analyzed by GAXRD, as shown in Figure S4. Diffraction profiles showed that 5 nm-thick In_2O_3 films were grown as nanocrystalline or amorphous films. The film thickness, roughness, and mass density of In_2O_3 PEALD films at the different stage temperatures were examined by XRR measurements, as presented in Figure 3b, and the film properties achieved are summarized in Table 2. The mass densities of In_2O_3 films prepared at 90, 180, and 250 °C were 6.64, 6.88, and 7.17 g/cm^3, respectively. Given the theoretical density of In_2O_3 (7.18 g/cm^3), the mass densities from XRR indicate the growth of very dense In_2O_3 films. The formation of dense In_2O_3 film was confirmed from refractive index of In_2O_3 films as described in the later part. The roughness below 1 nm demonstrated the smooth surface morphology of 19−24 nm-thick In_2O_3 films.

The surface morphologies of In_2O_3 films grown at 90 and 250 °C were observed over a scan area of 1 μm × 1 μm by AFM, as shown in Figure 4a and b, respectively. Fine and dense grains of In_2O_3 films could be confirmed at 250 °C, but clear grain structure was not found for 90 °C-deposited In_2O_3 film due to amorphous or nanocrystalline structure. An RMS roughness of ∼0.15−0.21 nm suggests that very smooth In_2O_3 films were grown as deposited.

DOI: 10.1021/acsami.6b07332
ACS Appl. Mater. Interfaces 2016, 8, 26924−26931

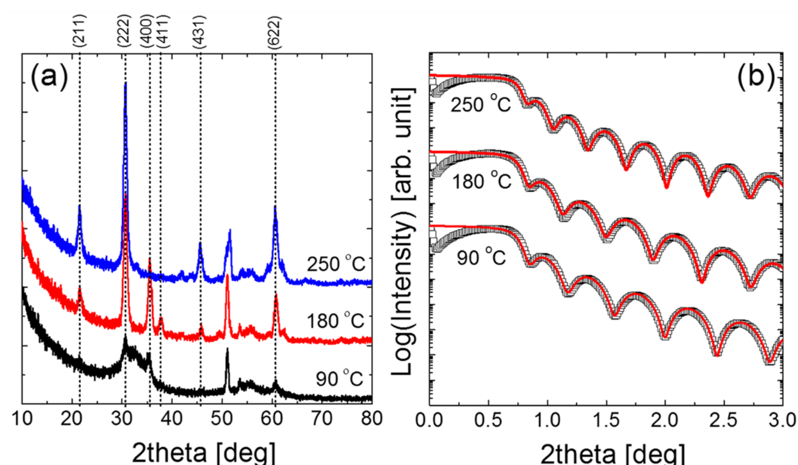

Figure 3. (a) GAXRD patterns of In_2O_3 films deposited on SiO_2 substrates for 300 cycles at growth temperatures of 90−250 °C. (b) XRR profiles of In_2O_3 films deposited on SiO_2 substrates with growth temperatures from 90 to 250 °C.

Table 2. Thickness, Mass Density, and Roughness of In_2O_3 PEALD Films at Deposition Temperatures of 90−250 °C

deposition temperature (°C)	thickness (nm)	mass density (g/cm^3)	roughness (nm)
90	18.9	6.64	0.82
180	20.2	6.88	0.99
250	23.6	7.16	0.87

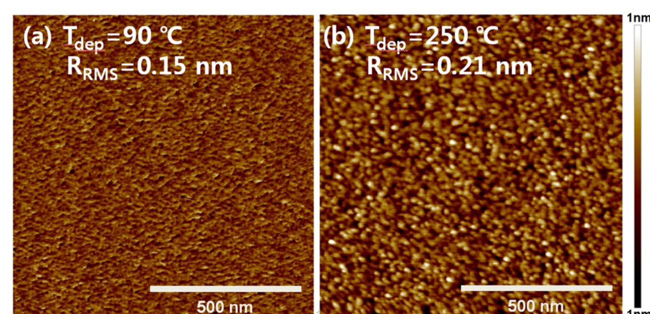

Figure 4. Surface morphologies of In_2O_3 films grown by PEALD at (a) 90 and (b) 250 °C.

Complex refractive indexes, $n + ik$, of the In_2O_3 films were measured by SE to extract the optical band gap and refractive index of the In_2O_3 films with deposition temperature. Here, the real part, n, and imaginary part, k, are the refractive index and the extinction coefficient of the In_2O_3 films, respectively. Figure 5a shows the variation in the optical band gap at various temperatures of 70−250 °C. The direct band gap was determined from the Tauc plot by extrapolating the linear region of $(\alpha h\nu)^2$ vs $h\nu$, where α and $h\nu$ are the absorption coefficient of In_2O_3 and the photon energy, respectively, as presented in the inset of Figure 5a. An In_2O_3 band gap of 3.6−3.8 eV was achieved, which is in good agreement with the reported band gap of In_2O_3.[11,19,21] In_2O_3 films grown at all temperatures of 70−250 °C showed sharp band edges. This suggests a low subgap state density of In_2O_3 films near the band edge, which is attributed to high-quality In_2O_3 films, independent of deposition temperature. In Figure S5, the refractive index of In_2O_3 films with varying wavelengths of light is presented. At 400−800 nm, the refractive index decreases with the wavelength of light, which agrees well with Cauchy's empirical equation. The refractive index of 2.0−2.1 was found at a wavelength of 577 nm for all investigated growth temperatures. Achieved refractive index is almost comparable

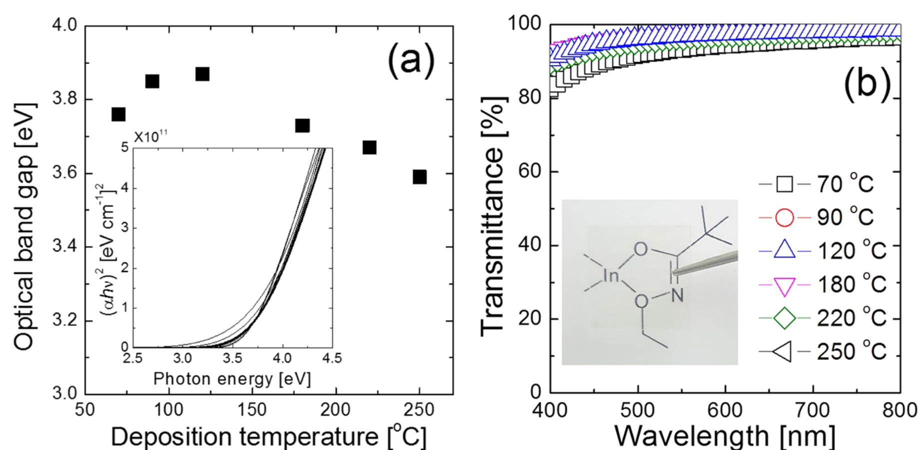

Figure 5. (a) Optical band gap of In_2O_3 films at various growth temperatures of 70−250 °C. The inset shows the Tauc plots for In_2O_3 films. (b) Transmittance of In_2O_3 films grown on glass substrates at deposition temperatures of 70−250 °C. The inset image is the transparent TFTs fabricated on glass substrates with In_2O_3 channel layers.

DOI: 10.1021/acsami.6b07332
ACS Appl. Mater. Interfaces 2016, 8, 26924−26931

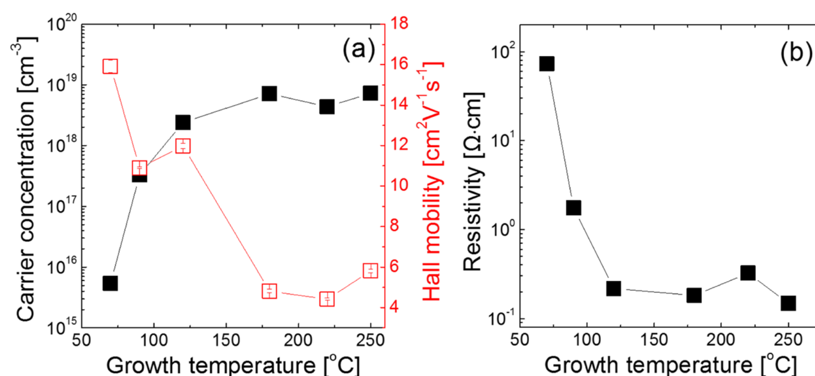

Figure 6. (a) Variations in carrier concentration and Hall mobilities of ∼20 nm-thick In_2O_3 films versus growth temperatures from 70 to 250 °C. (b) Resistivity of ∼20 nm-thick In_2O_3 films as a function of growth temperature.

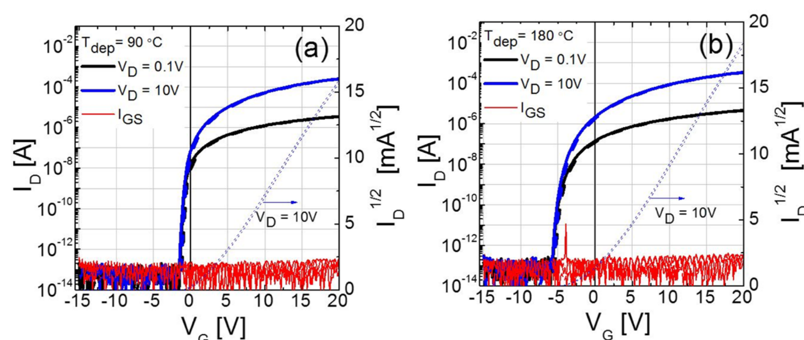

Figure 7. Transfer curves of TFTs with 5 nm-thick In_2O_3 films grown at (a) 90 and (b) 180 °C.

to that of single-crystal In_2O_3, implying the formation of dense In_2O_3 films. A visible range spectrometer was utilized to examine the transmittance of ∼20 nm-thick In_2O_3 films, as shown in Figure 5b. In_2O films showed a transmittance over 80% over the entire wavelength range. As shown in the inset image, TFTs fabricated with In_2O_3 channels showed sufficiently high transparency, which allows In_2O_3 film to be employed in various transparent device applications.

The electrical properties, including the carrier concentration, Hall mobility, and resistivity, of ∼20 nm-thick In_2O_3 films grown on glass substrates at deposition temperatures of 70−250 °C were investigated using Hall measurements, as presented in Figure 4. All films showed negative Hall coefficients, indicating n-type conduction of the In_2O_3. The electron concentration of the In_2O_3 films was influenced by the deposition temperature; in the relatively low deposition temperature regime, the carrier concentration of In_2O_3 PEALD films increased from 2×10^{17} to 4×10^{18} cm^{-3} with an increase in the growth temperature from 70 to 120 °C. Above 180 °C, all polycrystalline In_2O_3 films showed an almost constant carrier concentration about 5×10^{18} cm^{-3}, independent of the deposition temperature. The carrier concentrations of In_2O_3 films achieved in this work are significantly lower than that of reported In_2O_3 films prepared by sputtering, evaporation, and ALD using other In precursors.[11,12,16,20] This might be attributed to the high quality of the In_2O_3 films with low concentrations of electron donor defects (i.e., oxygen vacancies and In interstitials) and/or the fine-grained structure. Although there have been many efforts to suppress the electron concentration of In_2O_3 close to the semiconducting level by doping cations such as Ga, Si, and W, the growth of semiconducting In_2O_3 films by deposition at low temperature without doping has not yet been reported.[7,24] In addition, the Hall mobility of In_2O_3 films decreased from 16 to 6 $cm^2/V{\cdot}s$ with increasing growth temperature. The achieved Hall mobilities in this study are comparable with those of In_2O_3 films from $Et_2InN(TMS)_2/H_2O$ and DADI/H_2O.[20,21] The decrease in Hall mobility with growth temperature may be closely related to the evolution of the microstructure from amorphous or nanocrystalline films to polycrystalline films. As incoherent interface between amorphous and polycrystalline region as well as grain boundary can act as electron scattering center, the Hall mobility can be decreased as increasing deposition temperature.[25,26] According to the inverse relation between the carrier concentration and the resistivity, the resistivity of In_2O_3 films decreased from 72.4 to 0.15 Ω·cm with an increase in deposition temperature from 70 to 250 °C, as presented in Figure 6b. Because of the relatively low carrier concentration levels, the achieved resistivity was 1−2 orders of magnitude higher compared to the resistivity of In_2O_3 films reported in the literature.[16,19]

Although there are many reports on the In_2O_3-based TFTs using various fabrication methods of In_2O_3 channel layer such as ion beam deposition, CVD, solution-process, and sputter, a limited number of studies on ALD-grown In_2O_3-based TFT has been demonstrated.[4,8,27−29] In this work therefore the TFTs with 5 nm-thick In_2O_3 films deposited at 90−180 °C were fabricated, and their transfer characteristics were measured with and without cure annealing at 350 °C in O_2 atmosphere at drain voltages (V_D) of 0.1 and 10 V by sweeping the gate voltage (V_G) between −15 and 20 V, as shown in Figure 7. TFTs without cure annealing showed no field effect conductance switching, whereas all annealed TFTs presented excellent gate controllability in depletion mode with an on/off

current ratio (I_{on}/I_{off}) of about 10^9. With >10 nm In_2O_3 films or 250 °C deposited In_2O_3 films, however, it was unsuccessful to achieve desired transfer characteristics even after cure annealing, which might be due to the high carrier concentration of the active layer as shown in Figure S6. This is consistent with previous report by Jiao et al., that thinner In_2O_3 channel layer results in better transfer performance with higher I_{on}/I_{off}.[27] All retrieved TFT parameters of 90−180 °C grown In_2O_3-based TFTs including the turn-on voltage (V_{on}), subthreshold swing (SS), interface trap density (N_t), ΔV_{th}, and mobilities in linear and saturated regime (μ_{lin} and μ_{sat}), are summarized in Table 3.

Table 3. TFT Parameters for Different Deposition Temperatures of In_2O_3 Channels

						mobility ($cm^2/V{\cdot}s$)	
T_{dep} (°C)	V_{on} (V)	SS (V/dec)	N_t (cm^{-2})	ΔV_{th} (V)	I_{on}/I_{off}	μ_{lin}	μ_{sat}
90	−1.0	0.17	1.2×10^{12}	0	10^9	29	18
120	−1.3	0.21	1.4×10^{12}	0.14	10^9	28	16
180	−5.2	0.30	2.0×10^{12}	0.14	10^9	30	19

The V_{on} was defined as the value of gate voltage corresponding to a drain current of $(W/L) \times 10^{-11}$ A. The field effect mobilities were extracted from transconductance value (= dI_D/dV_G) at V_{on} + 15 V. The low ΔV_{th} of <0.14 V and low SS values of 0.17−0.3 V/decade of the fabricated TFTs imply a low trap density at the In_2O_3/Al_2O_3 interface as well as high-quality In_2O_3 channel layer. N_t was calculated from SS, and increased from 1.2×10^{12} to 2.0×10^{12} cm^{-2} with increasing growth temperature of In_2O_3 film. The V_{on} was shifted to negative voltage from −1.0 to −5.2 V as increasing growth temperatures of the In_2O_3 films, which might be ascribed to the lower resistivity of the In_2O_3 film at the higher deposition temperature. High field effect mobilities of 28−30 and 16−19 $cm^2/V{\cdot}s$ were obtained in the linear and saturated regime, respectively. Positive and negative bias-temperature stability of 90 °C-grown In_2O_3-based TFTs was examined under positive and negative bias stress of 1.14 MV/cm at 60 °C (Figure S7). A small V_{on} shift of −2.1 and −0.14 V after positive and negative bias stress for 10 000 s, respectively, indicates excellent quality of In_2O_3 channel and/or In_2O_3/Al_2O_3 interface. The resulting transfer performances of ALD-grown In_2O_3 TFTs were superior compared to previous In_2O_3-based TFTs fabricated by other deposition techniques.

■ CONCLUSIONS

A new type of liquid In precursor, $Me_2In(EDPA)$, was successfully synthesized using alkoxycarboxylicamide ligands for ALD of In_2O_3. The $Me_2In(EDPA)$ precursor showed suitable properties for ALD, including existing in the liquid state at room temperature, good thermal vaporization characteristics, and sufficient thermal stability. High-quality In_2O_3 films were achieved with a $Me_2In(EDPA)/O_2$ plasma with a saturated growth rate of 0.053 nm/cycle at 90−180 °C. Because of the high reactivity between $Me_2In(EDPA)$ and O_2 plasma, a low-temperature ALD process below 100 °C could be realized. As-grown In_2O_3 films showed negligible impurity concentrations, smooth surface morphology, and high film densities of 6.64−7.16 g/cm^3. The carrier concentration of In_2O_3 films deposited at low temperatures of 70 and 90 °C showed semiconducting levels as low as 3×10^{17} cm^{-3}, whereas In_2O_3 films deposited at 120−250 °C exhibited 1 order of magnitude higher carrier concentrations of about 5×10^{18} cm^{-3}. To evaluate PEALD In_2O_3 films as a channel material, coplanar structure bottom-gate TFTs were fabricated. In_2O_3-based TFTs showed excellent switching properties in terms of I_{on}/I_{off}, SS, ΔV_{th}, V_{on}, and field effect mobility. The low temperature In_2O_3 PEALD process using novel $Me_2In(EDPA)$ precursor developed in this study appear to be very promising for not only high-mobility thin film transistors but also other applications. In addition, new types of bidentate alkoxycarboxylic amide ligands can be adopted to other metal precursor for ALD and CVD applications.

■ ASSOCIATED CONTENT

Supporting Information

The Supporting Information is available free of charge on the ACS Publications website at DOI: 10.1021/acsami.6b07332.

TGA of $Me_2In(EDPA)$ over a temperature range of 26−800 °C; thermal decomposition of $Me_2In(EDPA)$ precursor; C 1s and N 1s XP spectra of In_2O_3 films grown at 90, 180, and 250 °C; GAXRD profiles of the 5 nm-thick In_2O_3 films grown at 90 and 250 °C; refractive index of In_2O_3 films deposited at 90−250 °C; transfer curves of TFTs without and with O_2 annealing depending on the different In_2O_3 deposition temperatures; transfer curves of TFTs for 90 °C-deposited In_2O_3 during negative and positive bias temperature stress (PDF)

■ AUTHOR INFORMATION

Corresponding Authors

*E-mail: tmchung@krict.re.kr (T.-M.C.).
*E-mail: jhan@krict.re.kr (J.H.H.)

Author Contributions

All authors have given approval to the final version of the manuscript.

Notes

The authors declare no competing financial interest.

■ ACKNOWLEDGMENTS

We would like to acknowledge the financial support from the R&D Convergence Program of MSIP (Ministry of Science, ICT and Future Planning) and NST (National Research Council of Science & Technology) of Republic of Korea (Grant. Convergence Practical Research Project-13-18-KRICT).

■ REFERENCES

(1) Morosawa, N.; Nishiyama, M.; Ohshima, Y.; Sato, A.; Terai, Y.; Tokunaga, K.; Iwasaki, J.; Akamatsu, K.; Kanitani, Y.; Tanaka, S.; Arai, T.; Nomoto, K. High-Mobility Self-Aligned Top-Gate Oxide TFT for High-Resolution AM-OLED. *J. Soc. Inf. Disp.* **2013**, *21*, 467−473.
(2) Park, J. S.; Maeng, W.-J.; Kim, H.-S.; Park, J.-S. Review of Recent Developments in Amorphous Oxide Semiconductor Thin-Film Transistor Devices. *Thin Solid Films* **2012**, *520*, 1679−1693.
(3) Fortunato, E.; Barquinha, P.; Martins, R. Oxide Semiconductor Thin-Film Transistors: A Review of Recent Advances. *Adv. Mater.* **2012**, *24*, 2945−2986.
(4) Nayak, P. K.; Hedhili, M. N.; Cha, D.; Alshareef, H. N. High Performance In_2O_3 Thin Film Transistors Using Chemically Derived Aluminum Oxide Dielectric. *Appl. Phys. Lett.* **2013**, *103*, 033518.
(5) Chen, P.-C.; Shen, G.; Chen, H.; Ha, Y.-g.; Wu, C.; Sukcharoenchoke, S.; Fu, Y.; Liu, J.; Facchetti, A.; Marks, T. J.;

Thompson, M. E.; Zhou, C. High-Performance Single-Crystalline Arsenic-Doped Indium Oxide Nanowires for Transparent Thin-Film Transistors and Active Matrix Organic Light-Emitting Diode Displays. *ACS Nano* **2009**, *3*, 3383−3390.

(6) Choi, C.-H.; Han, S.-Y.; Su, Y.-W.; Fang, Z.; Lin, L.-Y.; Cheng, C.-C.; Chang, C.-h. Fabrication of High-Performance, Low-Temperature Solution Processed Amorphous Indium Oxide Thin-Film Transistors Using a Volatile Nitrate Precursor. *J. Mater. Chem. C* **2015**, *3*, 854−860.

(7) Mitoma, N.; Aikawa, S.; Ou-Yang, W.; Gao, X.; Kizu, T.; Lin, M.-F.; Fujiwara, A.; Nabatame, T.; Tsukagoshi, K. Dopant Selection for Control of Charge Carrier Density and Mobility in Amorphous Indium Oxide Thin-Film Transistors: Comparison between Si- and W-Dopants. *Appl. Phys. Lett.* **2015**, *106*, 042106.

(8) Leppäniemi, J.; Huttunen, O.-H.; Majumdar, H.; Alastalo, A. Flexography-Printed In_2O_3 Semiconductor Layers for High-Mobility Thin-Film Transistors on Flexible Plastic Substrate. *Adv. Mater.* **2015**, *27*, 7168−7175.

(9) Wang, C. Y.; Cimalla, V.; Romanus, H.; Kups, T.; Ecke, G.; Stauden, T.; Ali, M.; Lebedev, V.; Pezoldt, J.; Ambacher, O. Phase Selective Growth and Properties of Rhombohedral and Cubic Indium Oxide. *Appl. Phys. Lett.* **2006**, *89*, 011904.

(10) Mitoma, N.; Aikawa, S.; Gao, X.; Kizu, T.; Shimizu, M.; Lin, M.-F.; Nabatame, T.; Tsukagoshi, K. Stable Amorphous In_2O_3-Based Thin-Film Transistors by Incorporating Sio2 to Suppress Oxygen Vacancies. *Appl. Phys. Lett.* **2014**, *104*, 102103.

(11) Cho, S. Effects of Rapid Thermal Annealing on the Properties of In_2O_3 Thin Films Grown on Glass Substrate by Rf Reactive Magnetron Sputtering. *Microelectron. Eng.* **2012**, *89*, 84−88.

(12) Kaleemulla, S.; Reddy, A. S.; Uthanna, S.; Reddy, P. S. Physical Properties of In_2O_3 Thin Films Prepared at Various Oxygen Partial Pressures. *J. Alloys Compd.* **2009**, *479*, 589−593.

(13) Basharat, S.; Carmalt, C. J.; Barnett, S. A.; Tocher, D. A.; Davies, H. O. Aerosol Assisted Chemical Vapor Deposition of In_2O_3 Films from Me_3In and Donor Functionalized Alcohols. *Inorg. Chem.* **2007**, *46*, 9473−9480.

(14) Asikainen, T.; Ritala, M.; Leskelä, M. Growth of In_2O_3 Thin Films by Atomic Layer Epitaxy. *J. Electrochem. Soc.* **1994**, *141*, 3210−3213.

(15) Nilsen, O.; Balasundaraprabhu, R.; Monakhov, E. V.; Muthukumarasamy, N.; Fjellvåg, H.; Svensson, B. G. Thin Films of In_2O_3 by Atomic Layer Deposition Using $In(acac)_3$. *Thin Solid Films* **2009**, *517*, 6320−6322.

(16) Lee, D.-J.; Kwon, J.-Y.; Lee, J. I.; Kim, K.-B. Self-Limiting Film Growth of Transparent Conducting In_2O_3 by Atomic Layer Deposition Using Trimethylindium and Water Vapor. *J. Phys. Chem. C* **2011**, *115*, 15384−15389.

(17) Elam, J. W.; Martinson, A. B. F.; Pellin, M. J.; Hupp, J. T. Atomic Layer Deposition of In_2O_3 Using Cyclopentadienyl Indium: A New Synthetic Route to Transparent Conducting Oxide Films. *Chem. Mater.* **2006**, *18*, 3571−3578.

(18) Elam, J. W.; Libera, J. A.; Hryn, J. N. Indium Oxide ALD Using Cyclopentadienyl Indium and Mixtures of H_2O and O_2. *ECS Trans.* **2011**, *41*, 147−155.

(19) Ramachandran, R. K.; Dendooven, J.; Poelman, H.; Detavernier, C. Low Temperature Atomic Layer Deposition of Crystalline In_2O_3 Films. *J. Phys. Chem. C* **2015**, *119*, 11786−11791.

(20) Maeng, W. J.; Choi, D.-w.; Chung, K.-B.; Koh, W.; Kim, G.-Y.; Choi, S.-Y.; Park, J.-S. Highly Conducting, Transparent, and Flexible Indium Oxide Thin Film Prepared by Atomic Layer Deposition Using a New Liquid Precursor $Et_2InN(SiMe_3)_2$. *ACS Appl. Mater. Interfaces* **2014**, *6*, 17481−17488.

(21) Maeng, W. J.; Choi, D.-w.; Park, J.; Park, J.-S. Atomic Layer Deposition of Highly Conductive Indium Oxide Using a Liquid Precursor and Water Oxidant. *Ceram. Int.* **2015**, *41*, 10782−10787.

(22) Choi, M.-C.; Kim, Y.; Ha, C.-S. Polymers for Flexible Displays: From Material Selection to Device Applications. *Prog. Polym. Sci.* **2008**, *33*, 581−630.

(23) Kim, D.; Nam, T.; Park, J.; Gatineau, J.; Kim, H. Growth Characteristics and Properties of Indium Oxide and Indium-Doped Zinc Oxide by Atomic Layer Deposition. *Thin Solid Films* **2015**, *587*, 83−87.

(24) Parthiban, S.; Kwon, J.-Y. Role of Dopants as a Carrier Suppressor and Strong Oxygen Binder in Amorphous Indium-Oxide-Based Field Effect Transistor. *J. Mater. Res.* **2014**, *29*, 1585−1596.

(25) Kuznetsov, V. L.; O'Neil, D. H.; Pepper, M.; Edwards, P. P. Electronic Conduction in Amorphous and Polycrystalline Zinc-Indium Oxide Films. *Appl. Phys. Lett.* **2010**, *97*, 262117.

(26) Buchholz, D. B.; Ma, Q.; Alducin, D.; Ponce, A.; Jose-Yacaman, M.; Khanal, R.; Medvedeva, J. E.; Chang, R. P. H. The Structure and Properties of Amorphous Indium Oxide. *Chem. Mater.* **2014**, *26*, 5401−5411.

(27) Jiao, Y.; Zhang, X.; Zhai, J.; Yu, X.; Ding, L.; Zhang, W. Bottom-Gate Amorphous In_2O_3 Thin Film Transistors Fabricated by Magnetron Sputtering. *Electron. Mater. Lett.* **2013**, *9*, 279−282.

(28) Dhananjay; Cheng, S.-S.; Yang, C.-Y.; Ou, C.-W.; Chuang, Y.-C.; Chyi Wu, M.; Chu, C.-W. Dependence of Channel Thickness on the Performance of In_2O_3 Thin Film Transistors. *J. Phys. D: Appl. Phys.* **2008**, *41*, 092006.

(29) Vygranenko, Y.; Wang, K.; Vieira, M.; Nathan, A. Indium Oxide Thin-Film Transistor by Reactive Ion Beam Assisted Deposition. *Phys. Status Solidi A* **2008**, *205*, 1925−1928.